

THE FLOW IN A RECTANGULAR CAVITY ON AN AXISYMMETRIC BODY

V. BASKARAN

ASIG/GWD, Aeronautical Research Laboratory
Defence Science and Technology Organisation
PO Box 1500, Salisbury, SA 5108, AUSTRALIA

ABSTRACT

Experiments have been conducted at subsonic speed on a generic model consisting of a rectangular cavity situated on an axisymmetric cylinder fitted with an ogive nose. Exploratory measurements of flow in terms of surface pressure distributions and surface flow patterns on the walls of the cavity for a length to depth ratio (L/H) range of 2.8 to 11.2 are presented. The results show that the flow in the cavity is 'open' for $L/H \leq 5.6$ and 'closed' for $L/H \geq 8.4$. Dominant features in the flow patterns corresponding to both types of cavity flows are identified.

INTRODUCTION

Stealth of modern military aircraft requires carriage of stores in cavities in the fuselage and their ejection when necessary. The flow in a rectangular cavity is such that it obstructs easy release of stores and some means of overcoming this problem is of interest. One needs to know the features of the basic flow inside cavities first before attempting to circumvent the release problem. This is where the current study has its origin.

In the literature, the flow in a cavity, depending on its length to height ratio, L/H , is classified as either 'open' or 'closed' based on whether the flow reattaches on the floor of the cavity or not (see Emerson and Poll 1989 for a review). In a 'closed or shallow' cavity flow the shear layer after separation at the leading edge of the cavity reattaches on the floor. The demarcation between 'open' and 'closed' cavity flows is in general not precise in that the dividing value of L/H has a finite range and is reported to vary widely depending on the free stream Mach number, state of the shear layer ahead of the cavity and the length to width ratio. Wilcox (1990) found the flow to be 'closed' for $L/H > 13$ and 'open' for $L/H < 10$ in the Mach number range of 1.5 to 2.86 with an initial turbulent boundary layer. It was also found that the effect of reducing the width to depth ratio of a cavity is to changed flow from one type to the other. Plentovich (1990) found the flow in the cavity 'open' for $L/H = 4.4$ and 'closed' for $L/H = 11.7$ at subsonic and transonic speeds.

In the present investigation an axisymmetric body is chosen to house the cavity rather than a flat plate, idealising to a first approximation the fuselage of aircraft. There is no information available in the literature for the practically important case of flows in rectangular or finite width cavities imbedded in an axisymmetric configuration. It is questionable whether the classification of the flow based on the length to depth ratio of the cavity imbedded in a flat plate is applicable to axisymmetric geometry. Therefore, the need to

investigate the flow behaviour in a rectangular cavity on an axisymmetric body is obvious.

The results to be presented here show that L/H values at which different flow types occur are different from their two-dimensional counterparts. The flow visualization reveals a complex development of flow inside the cavity with widely varying features depending on the length to depth ratio.

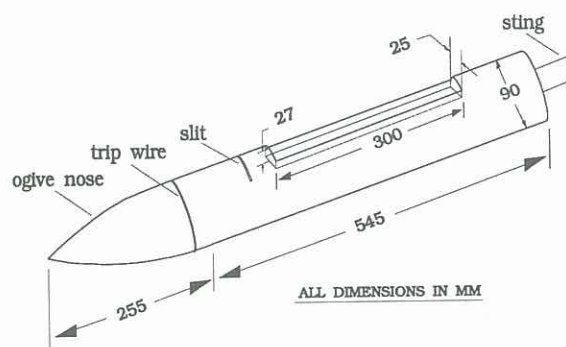


Figure 1. Cavity Model.

APPARATUS AND TECHNIQUES

Experiments were conducted on a generic model in the 300 mm x 380 mm low speed, low turbulence, open circuit wind tunnel at DSTO, Salisbury. The length of the working section was 1920 mm, and the tunnel was capable of operation up to a maximum test section speed of 50 m/s. The model consisted of a rectangular cavity imbedded in the surface of a 90 mm diameter hollow axisymmetric cylinder fitted with an ogive nose as shown in figure 1. The maximum length of the cavity was 300 mm. The length of the cavity was varied by inserting dummy blocks so that the effect of cavity geometry (length to depth ratio) could be studied on the flow. The maximum depth of the cavity was 27 mm and the width was 25 mm giving a width to depth ratio close to unity. Tests were made for four different length to depth ratios of 2.8, 5.6, 8.4, 11.2, at a tunnel speed of 48 m/s. The model was fitted with a 1.5 mm diameter trip wire at 10 mm ahead of the nose-centre body junction to simulate a turbulent boundary layer which exists ahead of the cavity on a full scale aircraft. The model was held along the centreline by means of a right-angled sting attached to the side wall of the tunnel working section.

Two identical but separate models, one for pressure measurement and the other for flow visualization of the cavity were used. Mean surface pressure distributions on all faces of the cavity were measured using the tappings provided on different faces of the cavity and a multichannel manometer. Surface flow inside the cavity was visualised using a mixture of titanium dioxide, castor oil and oelic acid.

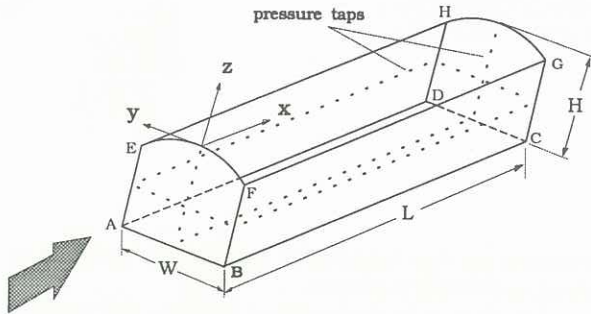


Figure 2. Labelled vertices of the cavity and axes.

RESULTS AND DISCUSSION

For each case of L/H , the pressure distributions on various faces of the cavity and corresponding surface flow patterns including an interpretation of the flow topology are presented together and discussed. The labelled vertices of the cavity and the co-ordinate system are shown in figure 2 so that the results on different faces can be referred to without ambiguity. Figures 3 to 6 show the results for the cavity with length to depth ratios of 11.2, 8.4, 5.6 and 2.8 respectively. The pressure coefficients were referenced to a value on the surface of the cylinder upstream of the cavity at $x = -74$ mm. The boundary layer thickness at $x = -74$ mm is approximately 6 mm giving a ratio of thickness to depth of about 0.22. The Reynolds number of the present experiments is 3.2×10^6 per meter.

Flow at $L/H = 11.2$ and 8.4 (figures 3 and 4)

The pressure coefficient, C_p , on the front face of the cavity AEFB reaches a constant value of about -0.18, before reaching a minimum value of -0.2 on the floor of the cavity at $x/L = 0.17$ ($x = 50$ mm). Further rise in C_p leads to a distinct maxima at $x/L = 0.33$ ($x = 100$ mm) on the floor ABCD and on the side walls AEHD and BFGC. Note that the physical location of the maximum C_p in the case with $L/H = 8.4$ still remains at $x = 100$ mm. In the case of the flow in the cavity with $L/H = 11.2$, C_p decreases and attains a minimum plateau on both floor and side walls, while in the case of $L/H = 8.4$ C_p remains more or less a constant up to $x/L = 0.62$ ($x = 140$ mm). This is expected as the flow has more room to expand into the longer cavity. All high subsonic and transonic investigations of Plentowich (1990) and supersonic cases of Wilcox (1990) do not exhibit any minima after the maximum C_p for the $L/H \geq 11$. The presence of the downstream face of the cavity causes the pressure to rise again to attain another plateau level near the corner of the floor and the rear face DHGC. C_p continues to rise on the rear face in both cases as the outer flow is approached, while it shows a slight variation across the rear face. The flow type in both cases can be classified clearly as 'closed' following earlier studies.

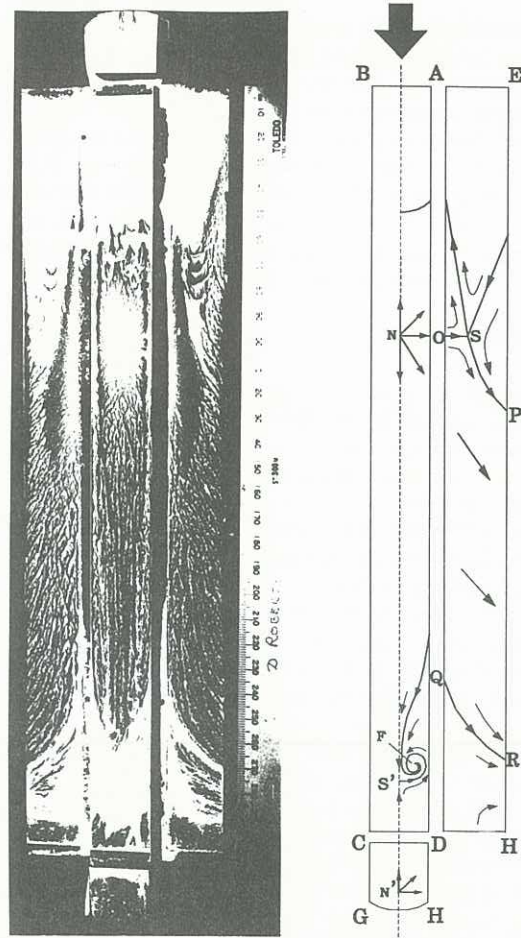
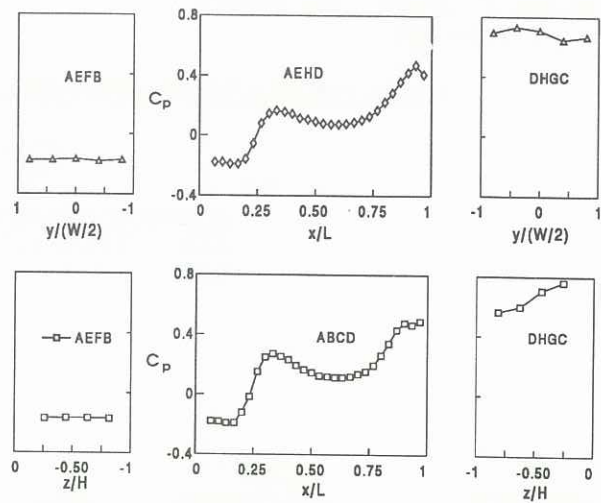


Figure 3. Surface pressure distributions and surface flow pattern for the cavity with $L/H = 11.2$.

The flow patterns for the two cases are very similar. The degenerate node N on the floor of the cavity can be related to the location of maximum C_p which is typical of reattaching shear layers. On the side walls the maxima corresponds to a point in close proximity to the saddle S . The region between the line spanning the node and the saddle, and the front face AEFB is the recirculating region. The flow on the floor downstream of the node converges and spirals in to form a focus on either side of the centreline giving in plan view a mushroom like pattern which is the main feature of

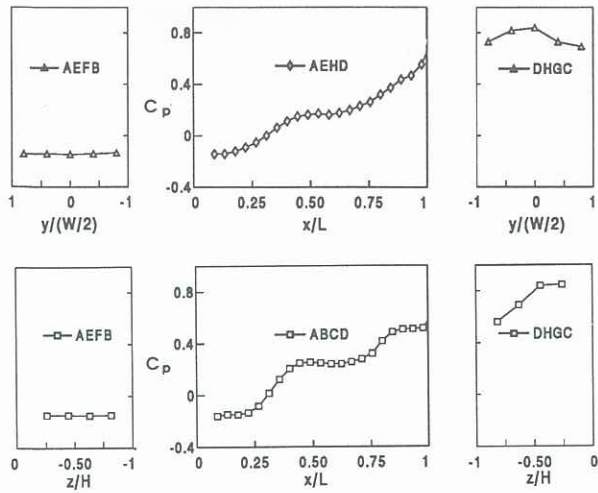


Figure 4. Surface pressure distributions and surface flow pattern for the cavity with $L/H = 8.4$.

the separation region ahead of the rear face DHGC. The focus can be seen to entrain the fluid partly from the region between the saddle S' on the top of the mushroom and the node N on the rear face (only shown in fig. 3), and also from sidewalls especially the region close to the floor behind the separatrix QR . The details of the flow topology behind QR are not clear from the photo. The fluid collected at the focus is expelled from the cavity in the form of a tornado to obey mass conservation. The flow on the side walls between the separatrices OSP and QR rolls up to form two counter rotating vortices with a downward common flow. These vortices trail along the edges of the cavity and form another complex pattern on the cylinder (not shown) behind the vertices G and H .

Flow at $L/H = 5.6$ (figure 5)

The pressure coefficient is close to zero (slightly positive) and varies uniformly on the forward face, AEFB. On the floor and the sidewalls C_p remains closely zero up to x/L of about 0.5 ($x = 75$ mm) before a rise to a value of 0.2 at the downstream end of the respective faces. The pressure distribution on the floor at this L/H corresponds to the 'open' type of cavity flow in the literature. On the rear face DHGC the pressure increases outwards and varies nonuniformly across the face. An oblique view of the cavity looking down and towards the side wall and floor is shown with the flow switched on. The flow pattern is symmetrical about the floor centreline. The flow on the floor is divided into two regions by the accumulation of oil at around $x = 85$ mm. The boundary of this accumulated region is in fact curved upstream. The disappearance of the oil on the floor downstream of oil accumulation suggests the flow on the floor ahead of the rear face is moving upstream. The flow on the side wall spirals in and forms a focus F near the floor of the cavity and the

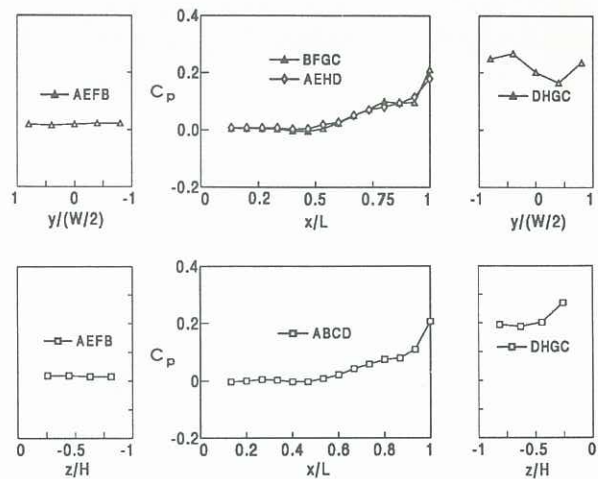


Figure 5. Surface pressure distributions and surface flow pattern for the cavity with $L/H = 5.6$.

accumulation of the oil can be clearly seen including some of the spiralled surface streamlines. In fact the fluid on the cylinder close to the cavity's edge is entrained into the focus from upstream and the affected region on the cylinder can be clearly seen enclosed by a curved separatrix stretching the whole length of the cavity. The flow is expected to be expelled outwards from the foci on both side walls to obey continuity. The conjecture here is that the tornados are bent and deflected downstream and then expelled towards the outer flow. The flow pattern indicates that the separated shear layer, while tending to expand into the cavity, is influenced by the rear face in such a manner as to deflect the shear layer towards the outer flow. This results in an 'open' type cavity flow.

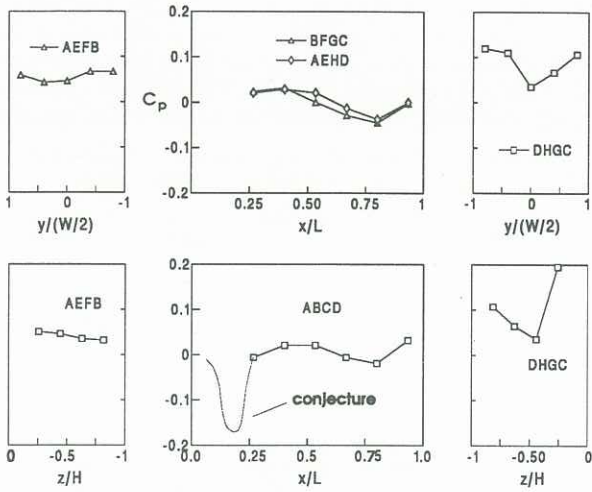


Figure 6. Surface pressure distributions and surface flow pattern for the cavity with $L/H = 2.8$.

Flow at $L/H = 2.8$ (figure 6)

The pressure coefficient on the upstream face is positive varying from 0.045 at the top to 0.03 as the floor is approached. Unlike other cases, the base pressure distribution across the front face is nonuniform. C_p remains close to zero on the floor and the side walls before an increase to a value of 0.1 at the bottom of the rear face. The pressure distributions on the side walls exhibit a slight difference between each other implying flow asymmetry. The pressure coefficient up and across the rear face exhibits a minimum at the centre. The photos showing the flow were shot while the flow was on since stopping the tunnel spreads the oil. The flow shows an unexpected but spectacular feature in the form of a strong vortex at $x = 15$ mm ($x/L = 0.2$). The vortex entrains fluid from almost everywhere inside the cavity and an accumulation of a significant portion of the oil painted on the different faces of the cavity can be seen at the eye of the vortex as a blob, including some of the separatrices along which the oil has flowed. The mechanism behind the vortex formation inside the cavity is not clear. The fluid within the vortex is expelled out of the cavity to obey continuity and can be conjectured to deflect the oncoming shear layer upwards. This could possibly explain why the base pressure is positive on the front face. Plentovich (1990) observed a positive value for the base pressure in a cavity with $L/H = 4.4$ at $M = 0.6$ fitted with a fence at the leading edge of a cavity which deflected the shear layer upwards. In the literature mention is often made that the flow is acoustically driven in a deep cavity and fluid dynamically driven in a shallow cavity. The present finding of a vortex formation suggests that the flow within the cavity with $L/H = 2.8$ is still fluid dynamically dominated.

CONCLUSIONS

The results of the present investigation lead to the following conclusions.

The classification of a flow in a cavity based on the length to depth ratio on an axisymmetric body is different from that reported in an embedded cavity on a flat plate. Present pressure distribution results classify the cavity flow as 'open' for $L/H \leq 5.6$ and 'closed' for $L/H \geq 8.4$.

The dominant features of the flow on the walls of the cavity corresponding to different L/H values are identified using surface flow visualization. For the closed cavity flow, the pattern is characterised by a node on the floor and saddles on the side walls at reattachment and a pair of foci on the floor characterising the separated flow ahead of the rear face. The flow in general is characterised by foci in open type flow. In the present case, foci appear on the side walls for $L/H = 5.6$ and a vortex (focus) on the floor for $L/H = 2.8$.

REFERENCES

- EMERSON, D. R. and POLL, D. I. A. (1989), Computation of laminar flow over cavities, Final Report on MoD Research Agreement Number 2052/78/RAE (F).
- PLENTOVICH, E. B. (1990), Three-dimensional cavity flow fields at subsonic and transonic speeds, NASA TM-4209.
- WILCOX, F. J. Jr. (1990), Experimental measurements of internal store separation characteristics at supersonic speeds, Proceedings of the Stores Carriage, Integration and Release Conference, Royal Aero. Society, Bath, England.